

# Quantitative determination of the single-molecule detection regime in fluorescence fluctuation microscopy by means of photon counting histogram analysis

Raluca Niesner and Karl-Heinz Gericke<sup>a)</sup>

*Institut für Physikalische und Theoretische Chemie, Technische Universität Braunschweig, Hans-Sommer Strasse 10, 38106 Braunschweig, Germany*

(Received 7 July 2004; accepted 31 January 2006; published online 4 April 2006)

Fluorescence fluctuation experiments are performed in single-molecule detection regime if the fluorescence of at most one molecule is registered at a time. Although the significance of such experiments for investigations of complex nonergodic systems like those met in the biosciences has been stressed out by many scientists, the quantitative and accurate determination of the single-molecule detection regime received rather little attention. In this work we present a method based on the photon counting histogram (PCH) analysis, which enables the determination of the average number  $\bar{N}$  of molecules within the observation volume, for which only the fluorescence of individual molecules is detected at a time. Thus, the accurate design of fluorescence fluctuation experiments performed in single-molecule detection regime is possible. Demonstrative fluorescence fluctuation experiments based on two-photon excitation are performed on diluted solutions of coumarin 153, in order to verify the potential of the PCH analysis in experiments on the single-molecule detection level. If the mean number  $\bar{N}$  of molecules within the excitation volume is larger than 0.048, the probability to simultaneously detect the fluorescence of two or more molecules is no longer negligible, i.e., no single-molecule detection regime. If the mean number  $\bar{N}$  of molecules is lower than 0.0057, the detection limit of the method is reached, i.e., the fluorescence signal cannot be distinguished from the background. Consequently, the concentration of coumarin 153 characteristic for the single-molecule detection regime lies in the range 13–110 pmol/l for the given experimental conditions. We also investigate the influence of the molecular brightness, i.e., detected photons per fluorophore molecule and sampling time, on the single-molecule detection regime. © 2006 American Institute of Physics. [DOI: 10.1063/1.2179793]

## I. INTRODUCTION

The development of fluorescence fluctuation spectroscopy (FFS) techniques based on far-field microscopy, in which the fluorescence signal of single molecules or of ensembles of few molecules is detected, has a particular significance for the biosciences, since these techniques enable a very detailed insight in complex biological systems at ambient temperature.<sup>1–5</sup> The major advantage of the FFS methods against standard macroscopic procedures is that they yield a distribution of the investigated parameter and not only its statistical average.

If the system under study is ergodic, the same averaged value of the parameter of interest is obtained in macroscopic experiments, in FFS experiments on ensembles of few molecules, as well as in FFS experiments on single molecules. However, if the investigated system is nonergodic, these values differ, since certain molecular processes can be registered only if single molecules are observed one at a time, i.e., in FFS experiments performed in single-molecule detection regime.<sup>6</sup> Due to the heterogeneous cellular environment and to the complex structure of biomolecules, such nonergodic systems are rather often in the biosciences.<sup>7–10</sup> For instance,

in fluorescence correlation spectroscopy (FCS) experiments, in which the conformational fluctuations of DNA fragments are monitored, Rigler *et al.* stress out that, since the system under study is nonergodic, the relaxation rates of the heterogeneously distributed subfractions of DNA fragments can correctly be determined only if the DNA fragments are individually detected. Thereby, they express their concern about the possibility of monitoring the fluorescence of two fragments at the same time.<sup>11</sup> Moreover, the theoretical models employed in FFS techniques, e.g., FCS simulation approaches,<sup>12,13</sup> are single-particle models, i.e., they describe the statistics of individual molecules.<sup>6</sup> In ergodic systems, these hypothetical single-particle models well represent the dynamics of both ensembles of molecules as well as of single molecules. In nonergodic systems, this assumption is no longer true. Only the data registered in experiments performed in single-molecule detection regime can directly be compared with the results of theoretical single-particle approaches.<sup>6</sup>

Although the importance of single-molecule detection in the FFS techniques is obvious,<sup>14</sup> the quantitative determination of the single-molecule detection regime received little attention until now. Rigorously, FFS experiments are performed in single-molecule detection regime, if all the mea-

<sup>a)</sup>Fax: 0049/531 391 5396. Electronic mail: k.gericke@tu-braunschweig.de

surement time only the fluorescence of individual molecules is detected, i.e., if the maximum number  $N_{\max}$  of molecules, the fluorescence of which simultaneously contributes to the detected signal, is one. The parameter, which defines the single-molecule detection regime, is consequently  $N_{\max}$ . Since  $N_{\max}$  is hardly accessible experimentally, only the average number  $\bar{N}$  of molecules within the observation volume can be used as an indicator of the single-molecule detection regime. Here it is important to notice that  $\bar{N}=1$  does not indicate the single-molecule detection regime. Even if the average number  $\bar{N}$  of molecules present in the observation volume is smaller than 1, there is a probability that two, three, or more molecules are simultaneously monitored.<sup>7,10</sup>

To our knowledge a quantitative determination of  $\bar{N}$  characteristic for the single-molecule detection regime ( $N_{\max}=1$ ) has not been performed in FFS yet. Therefore, a FFS theoretical approach, in which  $N_{\max}$  and  $\bar{N}$  explicitly appear as parameters, is necessary.

The FFS techniques are based either on the analysis of fluorescence fluctuation dynamics, i.e., fluorescence correlation spectroscopy,<sup>1,10,13,15,16</sup> or on the analysis of fluorescence fluctuation amplitudes at the equilibrium, i.e., moment analysis of fluorescence intensity distribution<sup>17,18</sup> (MAFID) and the very similar techniques photon counting histogram (PCH) analysis<sup>19–21</sup> and fluorescence intensity distribution analysis (FIDA).<sup>22</sup> Thereby, fluorescence can be induced either by one-photon or by two-photon excitation of the chromophore molecules. In one-photon confocal experiments even low laser intensities are sufficient to achieve a high fluorescence signal and, thus, the photodamage of the sample at the focal plane is rather low. Whereas the advantages of the two-photon microscopy in biological investigations are an excellent intrinsic three-dimensional (3D) resolution, low photodamage at the out-of-focus regions, and a large penetration depth in tissue.<sup>23,24</sup>

In FCS approaches, the simulation of fluorescence fluctuation dynamics results in theoretical autocorrelation functions. These functions explicitly depend only on parameters which describe the molecular dynamics and photodynamics, e.g., diffusion coefficient, photobleaching rate or triplet state rate, and on the average number  $\bar{N}$  of molecules present in the excitation volume.<sup>1,12,13,16</sup> The maximal number  $N_{\max}$  of simultaneously fluorescing molecules does not explicitly influence the shape of the autocorrelation function.

The fluorescence fluctuation amplitudes at the equilibrium are best described by the photon counting distribution of the fluorescence signal. While in MAFID the simulation of this distribution is not optimal due to the arbitrary selection of ordinary and central moments of fluorescence fluctuations, the PCH analysis and FIDA offer reliable and very similar simulation approaches, which differ only slightly in the mathematical formalism.

In the PCH analysis, i.e., a method based on the theory of photon detection, the statistics of fluorescence fluctuation amplitudes at the equilibrium is restored by a super-Poissonian (bistochastic) distribution of the photon counts.<sup>19</sup> This photon counting distribution is theoretically defined as a convergent series of terms which describe the photon count-

ing statistics of one, two, or more fluorescing molecules present in the observation volume.<sup>19,20</sup> The parameters, which influence the distribution of a single fluorescent species, are the molecular brightness  $\varepsilon$ , i.e., number of photons emitted by a molecule during a sampling period, and the average number  $\bar{N}$  of molecules in the observation volume.<sup>19</sup> This series can numerically be evaluated by summing up to the maximal number  $N_{\max}$  of molecules, the fluorescence of which simultaneously contributes to the detected signal, i.e., up to  $N_{\max}$  for which the series converges to its limit. Physically, the calculation of the series up to infinity describes the situation in which the fluorescence signal emitted by the sample is registered over an infinite time with an infinitesimal time resolution, so that there is a probability of simultaneously monitoring even an infinite number of molecules. However, under real circumstances, both the measurement time and the time resolution are finite and only the relevant fluorescence of  $N_{\max}$  molecules contribute to the detected signal. Thus, the shape of the simulated photon counting histogram in the PCH analysis is explicitly influenced by both the average number  $\bar{N}$  of molecules within the observation volume and the maximal number  $N_{\max}$  of simultaneously fluorescing molecules. Consequently, the PCH analysis is the appropriate FFS technique for a quantitative determination of  $\bar{N}$  in the single-molecule detection regime.

We apply for the first time the photon counting histogram analysis to quantitatively determine the single-molecule detection regime and discuss the influence of biologically relevant values of the molecular brightness on  $\bar{N}$  in this regime. Thereby, the single-molecule detection limit and the detection limit (background) defined as the upper, respectively, the lower limit of the single-molecule detection regime are determined by comparing the experimental uncertainty with the deviation between the super-Poissonian fluorescence distributions calculated up to  $N_{\max}=1$  and  $N_{\max}=2$ , respectively, and with the deviation between the Poissonian background distribution and the super-Poissonian fluorescence distribution calculated up to  $N_{\max}=1$ , respectively.

In order to verify the reliability of the PCH analysis on the single-molecule detection level, we performed two-photon excitation experiments on low concentration solutions of coumarin 153, i.e., an ergodic system, and approximate the resulting photon counting histograms of the fluorescence signal with the theoretically calculated super-Poissonian distributions. Moreover, the molecular brightness  $\varepsilon$  obtained in these experiments is exemplarily employed to determine  $\bar{N}$  in the single-molecule detection regime under the given experimental conditions.

The quantitative determination of the single-molecule detection regime described in this work is generally valid for all FFS techniques and allows the control of the experimental parameters, i.e., chromophore concentration, laser power, and excitation wavelength, for an accurate design of single-molecule detection experiments.

## II. PHOTON COUNTING STATISTICS

Let us consider that one or few molecules, which dwell in a small region around the laser focus, i.e., in the observation volume, are excited into the first ( $S_1$ ) or a higher ( $S_n$ ) singlet state, relax into the energetically lowest vibrational state of  $S_1$  and, by subsequent fluorescence, into the ground state  $S_0$ . The absorption-fluorescence cycles can be interrupted by transport processes, e.g., diffusion, or by photo-physical processes, e.g., photobleaching or intersystem crossing.<sup>16</sup> The fluctuations of the detected fluorescence signal contain information about molecular parameters, which can be extracted by means of PCH analysis as demonstrated by Chen *et al.*<sup>19</sup> and Mueller *et al.*<sup>20</sup>

The photon counting statistics of the fluctuating fluorescence signal is accurately described in a semiclassical manner by Mandel's formula.<sup>19,20</sup> Thereby, two random processes determine the shape of the photon counting distribution. The first process reflects the statistical independence of the photoelectric detection process for coherent electromagnetic radiation (the noise of the detector) restored by a Poissonian distribution. The second source of randomness is the fluorescence process itself. Consequently, since the Poissonian distribution of a light source, which emits a constant signal in time and space, is broadened if the emitted signal fluctuates, the photon counting histogram of the detected fluorescence signal is given by a super-Poissonian distribution, i.e., bistochastic distribution.

The fluctuations of the emitted fluorescence signal are caused by two factors.

- The spatially nonuniform illumination of the excitation volume given by the point spread function, PSF ( $r, z$ ).
- The variation of the number  $N$  of molecules within the excitation volume due to transport and photoprocesses, which is restored by the Poissonian distribution  $\text{Poi}(\bar{N}, N)$ . Here  $\bar{N}$  is the number of molecules within the excitation volume averaged over the entire measurement duration.

Considering these sources of fluorescence fluctuation, the photon counting distribution of the detected fluorescence signal is given by the sum over all photon counting distributions  $p_N(k; V_0, \varepsilon)$  weighted with the corresponding Poissonian terms  $\text{Poi}(\bar{N}, N)$ ,<sup>19</sup>

$$\Pi(k; \bar{N}, \varepsilon) = \sum_{N=0}^{\infty} p_N(k; V_0, \varepsilon) \text{Poi}(\bar{N}, N), \quad (1)$$

with  $N$  the number of molecules present at a time in the excitation volume  $V_0$  and  $\varepsilon$  the molecular brightness, i.e., number of photons emitted by a molecule during a sampling period  $T$ .

The function  $p_N(k; V_0, \varepsilon)$  describes the photon counting distribution of the fluorescence signal originating from  $N$  molecules and is calculated as the  $N$ -fold convolution of  $p_1(k; V_0, \varepsilon)$ , i.e., the photon counting distribution of the fluorescence signal of a single molecule.<sup>19</sup> In the case of two-photon excitation, for which the point spread function can be approximated by a two-dimensional (2D) Gauss-Lorentz dis-

tribution, the function  $p_1(k; V_0, \varepsilon)$  is defined as in Ref. 19. The function  $p_1(k; V_0, \varepsilon)$  calculated for the confocal one-photon fluorescence fluctuation microscopy is given in Refs. 25 and 26.

The function  $p_0(k; V_0)$  represents the Poissonian distribution  $\text{Poi}(\bar{k}, k)$  of the background photons with  $\bar{k}$  the average number of background photons detected during a sampling period  $T$ .

Concluding, the normalized distribution  $\Pi(k; \bar{N}, \varepsilon)$  for one fluorescing species depends only on two parameters: the molecular brightness  $\varepsilon$  and the average number  $\bar{N}$  of molecules present in the excitation volume.<sup>19,20</sup>

Numerically, the function  $\Pi(k; \bar{N}, \varepsilon)$  cannot be calculated up to infinity. Since  $\Pi(k; \bar{N}, \varepsilon)$  is a convergent series, it can accurately be evaluated by summing up to a maximum number  $N_{\max}$  of molecules simultaneously present in the excitation volume, the fluorescence of which still has a significant contribution to the detected signal.

$$\Pi(k; \bar{N}, \varepsilon, N_{\max}) = \sum_{N=0}^{N_{\max}} p_N(k; V_0, \varepsilon) \text{Poi}(\bar{N}, N). \quad (2)$$

Thus, beside the molecular brightness  $\varepsilon$  and the average number of molecules  $\bar{N}$  within the excitation volume, another parameter influences the distribution  $\Pi(k)$ , i.e., the maximum number  $N_{\max}$  of fluorescing molecules simultaneously present in the observation volume.  $N_{\max}$  is the quantitative indicator of the single-molecule detection regime and, thus, of particular significance. The deviation between the distribution  $\Pi(k; \bar{N}, \varepsilon)$  calculated up to  $N_{\max}=1$  and up to  $N_{\max}=2$ , respectively, is in the case of single-molecule detection equal to 0, i.e., the series  $\Pi(k; \bar{N}, \varepsilon, N_{\max})$  already converges to its limit for  $N_{\max}=1$ . A pragmatic approach, which is essential in experimental investigations, defines that the single-molecule detection regime is reached if the deviation between  $\Pi(k; \bar{N}, \varepsilon, N_{\max}=1)$  and  $\Pi(k; \bar{N}, \varepsilon, N_{\max}=2)$  does not exceed the experimental uncertainty.

## III. EXPERIMENT

The basic setup used to register the fluorescence signal in the fluorescence fluctuation experiments is similar to that described by Mertz *et al.*<sup>24</sup> The characteristics of the pulsed laser beam are 200 fs pulse width and 76 MHz repetition rate. A microscopy objective Plan Neofluar (40 $\times$ , NA=1.3, oil immersion) of the company Carl Zeiss is used to focus the tenfold expanded laser beam into the sample. The dimensions of the effective two-photon excitation volume are for an excitation wavelength  $\lambda$  of 800 nm: secondary axis  $\omega_0=334$  nm at the focal plane ( $x$ - $y$  plane), principal axis  $z_c=1570$  nm on the optical axis ( $z$  direction), and volume  $V_0 \sim 0.74$  fl.<sup>27</sup> These values were validated in experiments with fluorescent latex microbeads for the  $x$ - $y$  resolution and with fluorescein isothiocyanate (FITC) monolayers for the  $z$  resolution.<sup>28</sup> As detection unit we use an avalanche photodiode (SPCM-AQ-131, EG&G Optoelectronics Canada), encompassing a total detection efficiency of 3% for coumarin 153 ( $\lambda_F=532$  nm). The signal of the avalanche photodiode is

directed to a multichannel scalar (MCD-2E, 7882, FAST ComTec) operated at 10 kHz (sampling period  $T=100 \mu\text{s}$ ). The total number of data points  $M$  is  $1.32 \times 10^5$ .

For the fluorescence fluctuation experiments we used solutions (50, 100, 200, and 400 pmol/l and 1 nmol/l) of coumarin 153 (Radiant Dyes) in glycol p.a.

#### IV. DATA ANALYSIS

If the deviation between the distributions  $\Pi(k; \bar{N}, \varepsilon, N_{\max}=1)$  and  $\Pi(k; \bar{N}, \varepsilon, N_{\max}=2)$  is equal to or lower than the experimental uncertainty, it can be assumed that the single-molecule detection regime is reached, i.e., the probability to simultaneously detect the fluorescence of two molecules is negligible.

The experimental uncertainty represents the difference between the normalized experimental data  $p_{\text{exp}}(k)$  and the calculated photon counting histogram  $\Pi(k; \bar{N}, \varepsilon)$  and is given

$$\chi^{2\#} = \frac{M^2}{k_{\max} - d} \sum_{k=0}^{k_{\max}} \left( \frac{\Pi(k; \varepsilon, \bar{N}, N_{\max}=1) - \Pi(k; \varepsilon, \bar{N}, N_{\max}=2)}{\sigma'} \right)^2. \quad (4)$$

Here, the standard deviation  $\sigma'$  is defined as  $\sigma' = \sqrt{M \Pi(k; \varepsilon, \bar{N}, N_{\max}=1) (1 - \Pi(k; \varepsilon, \bar{N}, N_{\max}=1))}$ .

Consequently, the single-molecule detection limit is mathematically described by the relation:  $\chi^{2*} = \chi^{2\#}$ . The factors which influence the  $\chi^{2\#}$  parameter, i.e., the single-molecule detection limit, are the average number  $\bar{N}$  of molecules within the excitation volume and the molecular brightness  $\varepsilon$ .

The deviation between the Poissonian distribution  $\text{Poi}(\bar{k}, k)$  of the background photons and the distribution  $\Pi(k; \bar{N}, \varepsilon, N_{\max}=1)$  given by the  $\chi^{2*}$  parameter and defined analogously to the  $\chi^2$  parameter indicates the detection limit of the experimental method,<sup>24</sup>

$$\chi^{2*} = \frac{M^2}{k_{\max}} \sum_{k=0}^{k_{\max}} \left( \frac{\Pi(k; \varepsilon, \bar{N}, N_{\max}=1) - \text{Poi}(\bar{k}, k)}{\sigma'} \right)^2. \quad (5)$$

If this parameter is lower than the experimental uncertainty, the emitted fluorescence signal cannot be distinguished from the background and, thus, cannot be detected.

Thus, the single-molecule detection regime is defined as the range between the upper single-molecule detection limit ( $\chi^{2\#} = \chi^2$ ) and the lower detection limit ( $\chi^{2*} = \chi^2$ ).

## V. RESULTS AND DISCUSSION

### A. PCH analysis of experimental data

The fluorescence signal of very diluted solutions of coumarin 153 in glycol is analyzed by means of PCH analysis in

by the  $\chi^2$  parameter. Assuming that the probability of observing  $k$  photons  $n$  times out of  $M$  trials is a binomial distribution, the  $\chi^2$  parameter is given by<sup>19,20</sup>

$$\chi^2 = \frac{M^2}{k_{\max} - d} \sum_{k=0}^{k_{\max}} \left( \frac{p_{\text{exp}}(k) - \Pi(k; \bar{N}, \varepsilon)}{\sigma} \right)^2. \quad (3)$$

Here,  $M$  is the total number of trials (data points),  $k_{\max}$  is the maximum number of photons detected during a sampling period  $T$ ,  $d$  is the number of fitting parameters ( $\varepsilon$  and  $\bar{N}$ ),  $p_{\text{exp}}(k)$  is the experimental probability of detecting  $k$  photons during a sampling period  $T$ , and  $\sigma$  is the standard deviation defined as  $\sqrt{M p_{\text{exp}}(k) (1 - p_{\text{exp}}(k))}$ . In addition to the reduced  $\chi^2$  parameter, the normalized residuals  $r(k) = M(p_{\text{exp}}(k) - \Pi(k; \bar{N}, \varepsilon)) / \sigma$  of the fitting procedure indicate the quality of the theoretical model.<sup>19,20</sup>

In order to quantify the deviation between the distributions  $\Pi(k; \bar{N}, \varepsilon, N_{\max}=1)$  and  $\Pi(k; \bar{N}, \varepsilon, N_{\max}=2)$  we define the  $\chi^{2\#}$  parameter analogously to the  $\chi^2$  parameter,

order to verify the reliability of this method in evaluating fluorescence fluctuations around the single-molecule detection limit. Moreover, in this way the experimental uncertainty restored by the  $\chi^2$  parameter is obtained, which is necessary for the quantitative determination of the single-molecule detection regime by means of PCH analysis.

The fluorescence signal of four solutions of coumarin 153 in glycol (50, 100, 200, and 400 pmol/l) was registered at a mean laser power  $\bar{P}=22$  mW and at an excitation wavelength  $\lambda=800$  nm. Under these conditions, no photobleaching or intersystem crossing occurs and, thus, the number of fluorescing molecules present in the excitation volume varies only due to diffusion.<sup>27</sup> The sampling time  $T=100 \mu\text{s}$  is short enough to track the fluctuations of the fluorescence signal induced by the diffusion of the fluorescing molecules through the excitation volume (average diffusion time determined in FCS experiments is 1.25 ms).<sup>27</sup> The mean background count rate of glycol, including a dark count rate of 200 Hz, amounts to 500 Hz. The experimental photon counting histograms of the detected fluorescence signals of the four solutions are approximated by simulated photon counting distributions  $\Pi(k)$ .  $N_{\max}$  is fixed to 50 molecules, a few hundred times larger than the average number  $\bar{N}$  of molecules present in the excitation volume in order to assure that all molecules, which might contribute to the detected fluorescence signal, are taken into account.

Figure 1 demonstrates that the experimental photon counting distributions are well approximated by the functions  $\Pi(k)$  ( $\chi^2$  amounts to approximately 2) and are signifi-

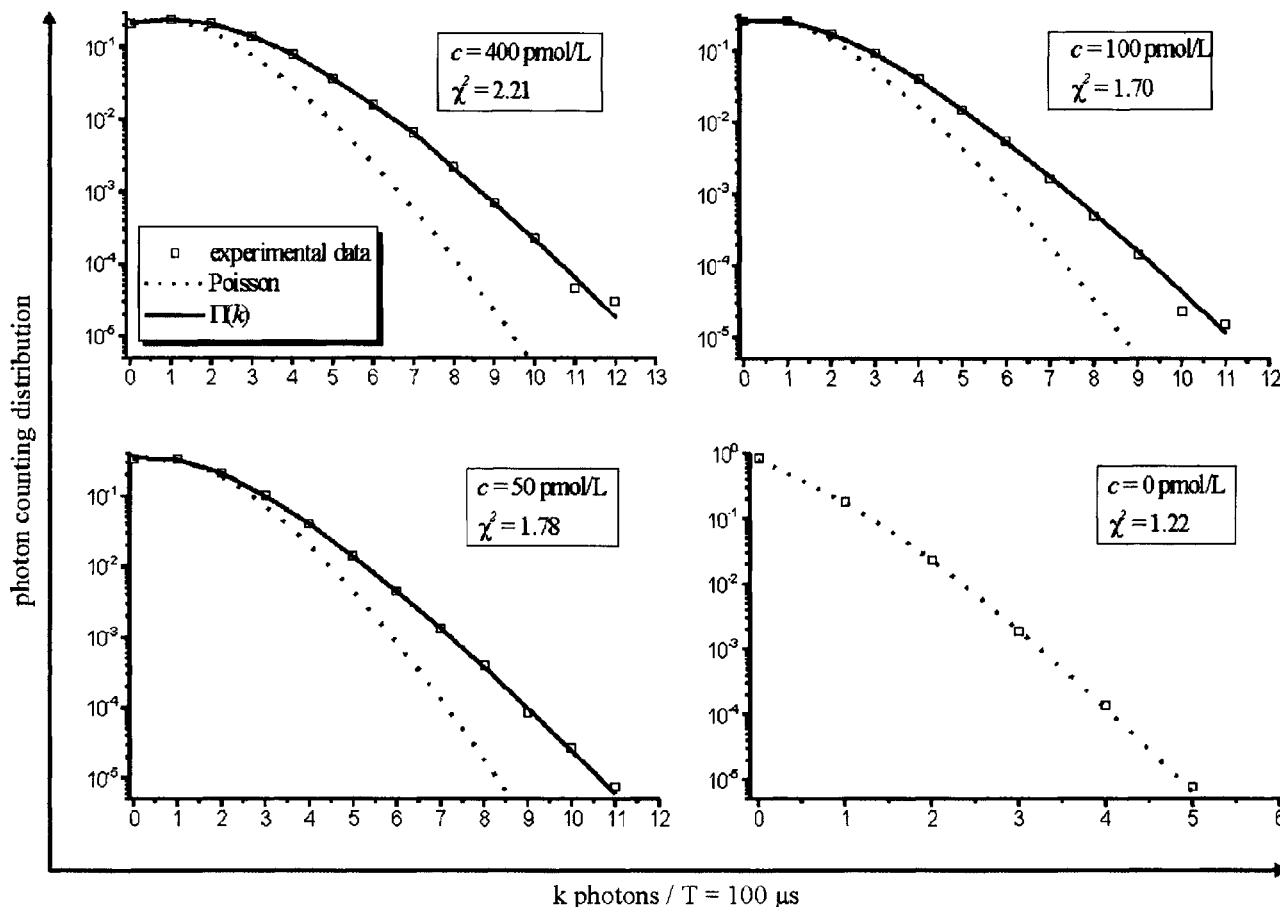


FIG. 1. Experimental photon counting distributions of the detected signal of three different solutions of coumarin 153 in glycol (400, 100, and 50 pmol/l) and of the solvent (glycol), calculated super-Poisson distributions  $\Pi(k)$ , and corresponding Poisson distributions. Experimental parameters:  $\bar{P}=22$  mW,  $\lambda=800$  nm. Parameters employed in the simulation of  $\Pi(k)$ :  $T=100$   $\mu$ s,  $N_{\max}=50$  molecules,  $M=1.32 \times 10^5$ . Fitted parameters:  $\varepsilon=1.21 \pm 0.2$  cpm;  $\bar{N}=0.024$  for  $c=50$  pmol/l,  $\bar{N}=0.047$  for  $c=100$  pmol/l, and  $\bar{N}=0.196$  for  $c=400$  pmol/l.

cantly broader than the corresponding Poissonian distributions. The photon counting distribution of the background signal is accurately approximated by a Poissonian distribution ( $\chi^2=1.22$ ). In all experiments the residuals  $r(k)$  oscillate around 0 with a maximal amplitude smaller than  $10^{-5}$  (data not shown).

By fitting the experimental photon counting distributions with the simulated functions  $\Pi(k)$  a molecular brightness  $\varepsilon$  of  $1.21 \pm 0.02$  cpm (counts per molecule and sampling time  $T$ ) was obtained for all four concentrations. A more general molecular parameter independent from the sampling time is the specific molecular brightness  $\varepsilon_T = \varepsilon/T$ , which amounts in this case to 12 100 cpms (counts per molecule and second). The average number  $\bar{N}_{\text{PCH}}$  of molecules within the excitation volume obtained in the same fitting procedure is in good agreement with both the average number  $\bar{N}$  of molecules within the excitation volume calculated from the bulk concentration of the solution  $\bar{N} = cV_0N_A$  and with results of fluorescence correlation spectroscopy (FCS) experiments (see Table I). In FCS experiments, the average number  $\bar{N}_{\text{FCS}}$  of molecules within the excitation volume can be acquired from the amplitude of the fluorescence autocorrelation functions.<sup>24</sup>

As expected, the parameter  $\bar{N}$  determined by means of

PCH analysis and that determined from the bulk concentration  $\bar{N} = cV_0N_A$  are larger than that determined by means of FCS, as shown in Table I.

The results presented in this section demonstrate the reliability of the theoretical PCH model to simulate the photon counting distribution of the fluctuating fluorescence signal around the single-molecule detection limit. Moreover, we obtain a typical experimental uncertainty  $\chi^2$  around 2 (see inset of Fig. 1).

TABLE I. The mean number  $\bar{N}$  of molecules within the excitation volume as it results from the bulk concentration of the solutions  $\bar{N} = cV_0N_A$ , from the approximation of the experimental photon counting distributions with the functions  $\Pi(k)$  ( $\bar{N}_{\text{PCH}}$ ) and from the analysis of the fluorescence autocorrelation functions ( $\bar{N}_{\text{FCS}}$ ).

$c$ [pmol/l]	$\bar{N} = cV_0N_A$	$\bar{N}_{\text{PCH}}$	$\bar{N}_{\text{FCS}}$
50	0.022	0.024	...
100	0.045	0.047	0.063
200	0.088	0.095	0.115
400	0.177	0.196	0.251

## B. Single-molecule detection regime

Rigorously defined, the single-molecule detection regime is reached if only the fluorescence of single molecules present in the excitation volume is detected at a time. In the following we will demonstrate how the single-molecule detection regime in fluorescence fluctuation experiments can quantitatively be determined by means of PCH analysis.

The photon counting histogram of the detected fluorescence signal originating from one or few molecules is restored by the series  $\Pi(k; \bar{N}, \varepsilon, N_{\max})$ . On the single-molecule detection level, only the fluorescence signal of individual molecules is detected and, thus, the series  $\Pi(k; \bar{N}, \varepsilon, N_{\max})$  already converges to its limit for  $N_{\max}=1$ . Consequently, the deviation between the distributions  $\Pi(k; \bar{N}, \varepsilon, N_{\max}=1)$  and  $\Pi(k; \bar{N}, \varepsilon, N_{\max}=2)$  quantified by the  $\chi^{2\#}$  parameter is negligible in the case of single-molecule detection. The other two parameters of the series  $\Pi(k; \bar{N}, \varepsilon, N_{\max})$ , i.e., the average number  $\bar{N}$  of molecules within the excitation volume and the molecular brightness  $\varepsilon$ , implicitly influence the  $\chi^{2\#}$  parameter and, thus, the upper limit of the single-molecule detection. We will first concentrate our attention on the influence of the average number  $\bar{N}$  of molecules present in the excitation volume on the  $\chi^{2\#}$  parameter and then on the influence of the molecular brightness  $\varepsilon$  on  $\chi^{2\#}$ .

Figure 2 shows the photon counting distributions  $\Pi(k; \bar{N}, \varepsilon, N_{\max})$  calculated for three different parameters  $\bar{N}$  and different  $N_{\max}$ . If the average number of molecules  $\bar{N}$  within the excitation volume is equal to 1, the maximum number  $N_{\max}$  of molecules which simultaneously contribute to the detected signal is significantly larger than 1 (up to 4 molecules) [Fig. 2(c)]. Even for  $\bar{N}=0.48$ ,  $N_{\max}$  is larger than 1 and the experimental photon counting distribution of the fluorescence signal of a 1 nmol/l coumarin 153 solution cannot be approximated by  $\Pi(k; \bar{N}=0.48, \varepsilon, N_{\max}=1)$  [Fig. 2(b)]. Only for  $\bar{N} \ll 1$ , the contribution of two simultaneously fluorescing molecules to the detected signal vanishes [Fig. 2(a)]. In this case, the theoretical function  $\Pi(k; \bar{N}=0.024, \varepsilon, N_{\max}=1)$  accurately approximates the experimental data (50 pmol/l coumarin 153 solution). The molecular brightness employed in the simulation is  $\varepsilon_T=12\,100$  cps.

Quantitatively, the upper single-molecule detection limit is mathematically defined by the relation  $\chi^{2\#}=\chi^2$ . Thus, the influence of the average number  $\bar{N}$  of molecules present in the excitation volume on the upper single-molecule detection limit is investigated by comparing the  $\chi^{2\#}$  parameter dependence on  $\bar{N}$  with the constant value of the experimental uncertainty  $\chi^2$  (in our experiments  $\chi^2$  is approximately 2). The function  $\chi^{2\#}(\bar{N})$  is calculated for a fixed molecular brightness  $\varepsilon_T=12\,100$  cps, i.e., the molecular brightness of coumarin 153 (C153) at  $\bar{P}=22$  mW and  $\lambda=800$  nm.

As Fig. 3 shows, the  $\chi^{2\#}$  parameter tends asymptotically to zero at low  $\bar{N}$  and increases superpolynomial for  $\bar{N}$  larger than 0.1 molecules. By comparing the function  $\chi^{2\#}(\bar{N})$  with the  $\chi^2$  parameter, i.e., experimental uncertainty, we find that

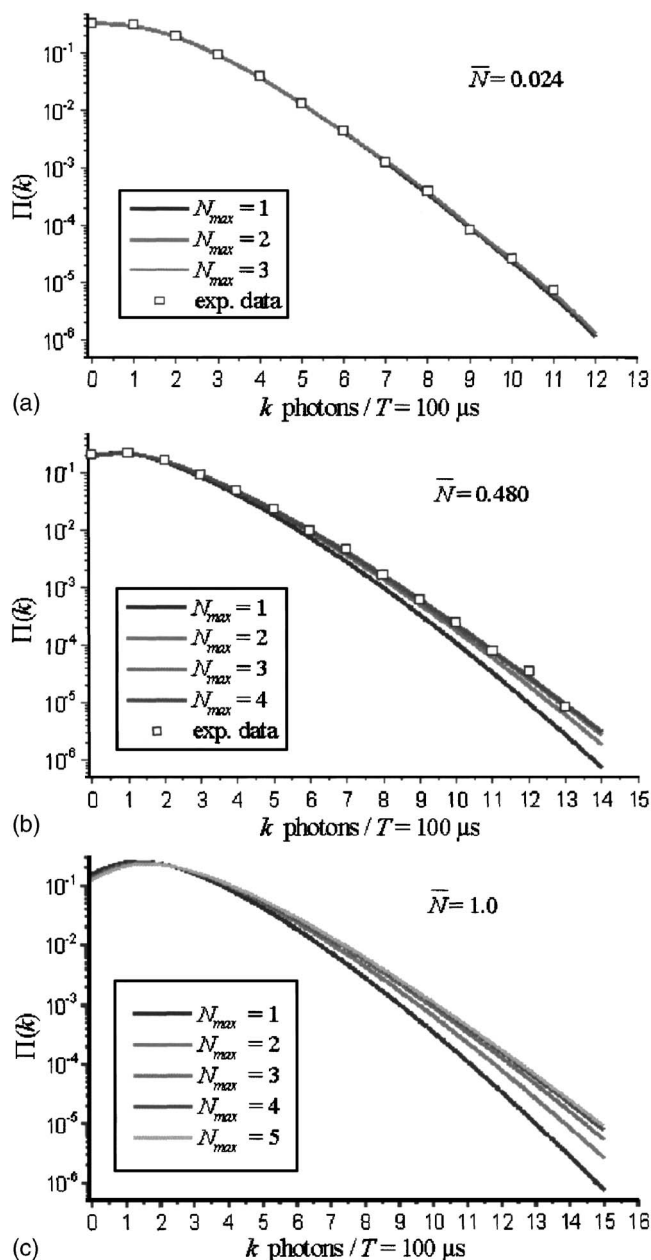


FIG. 2. (a) Experimental data of a 50 pmol/l solution of coumarin 153 in glycol and corresponding photon counting distributions  $\Pi(k; \bar{N}=0.024, \varepsilon, N_{\max})$  calculated for  $N_{\max}$  between 1 and 3 molecules. (b) Experimental data of a 1 nmol/l solution of coumarin 153 in glycol and corresponding photon counting distributions  $\Pi(k; \bar{N}=0.48, \varepsilon, N_{\max})$  calculated for  $N_{\max}$  between 1 and 4 molecules. (c) Photon counting distributions  $\Pi(k; \bar{N}=1, \varepsilon, N_{\max})$  calculated for  $N_{\max}$  between 1 and 5 molecules. The contribution of the fluorescence of more than one molecule to the detected signal is significant for  $\bar{N}=0.48$  (up to 3 molecules) and  $\bar{N}=1.0$  (up to 4 molecules) but negligible for  $\bar{N}=0.024$ . Parameters employed in the simulation:  $\varepsilon_T=12\,100$  cps.

the upper single-molecule detection limit is already reached at  $\bar{N}=0.048$  (or  $c \sim 110$  pmol/l for  $V_0=0.74$  fl) for  $\varepsilon_T=12\,100$  cps.

For  $\bar{N}$  below 0.0057 molecules ( $c \sim 13$  pmol/l for  $V_0=0.74$  fl) the deviation between the photon counting distribution  $\Pi(k; \bar{N}, \varepsilon, N_{\max}=1)$  and the Poisson distribution  $\text{Poi}(\bar{k}, k)$  of the background signal given by the  $\chi^{2*}$  parameter

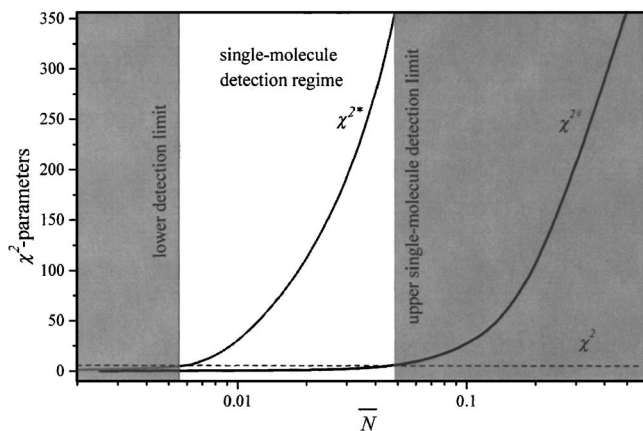


FIG. 3. The  $\chi^{2\#}$  parameter and the  $\chi^{2*}$  parameter as functions of the mean number  $\bar{N}$  of molecules within the excitation volume. By comparing the functions  $\chi^{2\#}(\bar{N})$ , respectively,  $\chi^{2*}(\bar{N})$  with the experimental uncertainty  $\chi^2$ , the upper single-molecule detection limit is determined to be at  $\bar{N} = 0.048$  molecules while the lower detection limit is reached at  $\bar{N} = 0.0057$  molecules. Parameters employed in the simulation:  $\varepsilon_T = 12\,100$  cpms,  $M = 10^6$ .

is lower than our experimental uncertainty  $\chi^2$ . Thus, below this level no detection is possible (see Fig. 3). Up to this point, the influence of the average number  $\bar{N}$  of molecules on the  $\chi^{2\#}$  parameter and on the  $\chi^{2*}$  parameter has been discussed only for a given molecular brightness. However, the molecular properties and the instrumental factors, i.e., the molecular brightness, significantly influence the dependence of these parameters on  $\bar{N}$  and on the regime of single-molecule detection. Consequently, we investigate the functions  $\chi^{2\#}(\bar{N})$  and  $\chi^{2*}(\bar{N})$  at different values of the molecular brightness  $\varepsilon_T$ , from 1625 to 30 000 cpms. These values cover the typical range of molecular brightness met in bio-scientific investigations.<sup>3,4,21</sup>

The comparison of the functions  $\chi^{2\#}(\bar{N})$  calculated for different values of  $\varepsilon$  with the experimental uncertainty  $\chi^2$  evidence that the mean number  $\bar{N}$ , at which the upper single-molecule detection limit is reached, increases with decreasing molecular brightness  $\varepsilon_T$  (Fig. 4). Consequently,  $\bar{N}$ , at which the upper single-molecule detection limit is reached, amounts to 0.007 molecules for a molecular brightness  $\varepsilon_T = 30\,000$  cpms while the same parameter for ten times lower molecular brightness  $\varepsilon_T = 3250$  cpms amounts to 0.42 molecules. The comparison of the functions  $\chi^{2*}(\bar{N})$  calculated for the same values of  $\varepsilon_T$  with the experimental uncertainty  $\chi^2$  reveals that  $\bar{N}$ , at which the fluorescence signal vanishes in the background (i.e., the detection limit), also increases with decreasing molecular brightness (data not shown).

Concluding, fluorescence of individual molecules is detected only in the range given by the lower detection limit ( $\chi^{2*} = \chi^2$ ) and the upper single-molecule detection limit ( $\chi^{2\#} = \chi^2$ ). The values of  $\bar{N}$  corresponding to these limits vary with the molecular brightness, however,  $\bar{N}$  at the lower detection limit is always smaller than  $\bar{N}$  at the upper single-molecule detection limit. Thus, experiments in single-

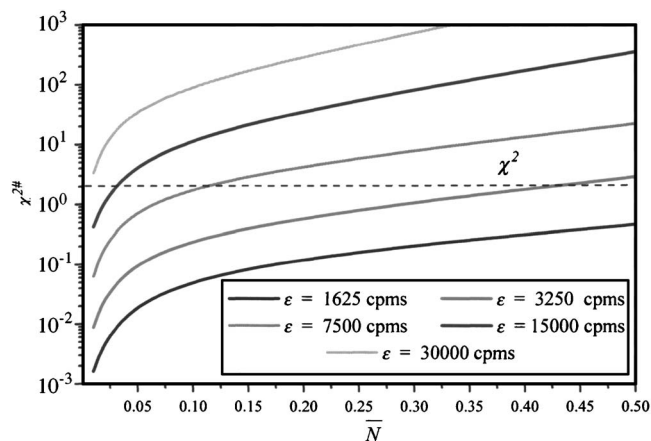


FIG. 4. The dependence of the  $\chi^{2\#}$  parameter on the mean number  $\bar{N}$  of molecules present in the excitation volume calculated for different values of the molecular brightness  $\varepsilon_T$ . Parameters employed in the simulation:  $T = 100$   $\mu$ s,  $M = 10^6$ .

molecule (SM) detection regime can generally be performed for all values of the molecular brightness, i.e., independent from the fluorescing species and under arbitrary instrumental conditions. However, since biological investigations should be carried out at low mean laser powers  $\bar{P}$  in order to avoid photodamage at the sample and since the molecular brightness quadratically scales with  $\bar{P}$ , relevant experiments are possible only for  $\varepsilon_T$  up to a maximal value determined by the maximal noninvasive mean laser power. On the other side the concentration of the fluorescing species (directly proportional to  $\bar{N}$ ) in the single-molecule detection regime is very large for low values of  $\varepsilon_T$ . A too large concentration of fluorescing species constitutes a significant disadvantage in biological studies, i.e., in labeling experiments, since this may lead to modifications of the natural environment and, thus, to altered results.

The quantitative determination of the single-molecule detection regime by means of PCH analysis is generally valid for all fluorescence fluctuation techniques. However, the SM regime is influenced by experiment specific factors like the experimental uncertainty and, thus, may slightly vary for different setups.

## VI. SUMMARY

We presented a novel application of the photon counting histogram (PCH) analysis, which enables the accurate design of fluorescence fluctuation experiments in single-molecule detection regime.

In the single-molecule detection regime the maximal number  $N_{\max}$  of molecules simultaneously fluorescing in the observation volume is equal to 1. Under these conditions, the photon counting histogram of the fluctuating fluorescence signal mathematically described by the function  $\Pi(k; \bar{N}, \varepsilon, N_{\max})$ , i.e., a convergent series in  $N_{\max}$ , already converges to its limit for  $N_{\max} = 1$ . The upper limit of the single-molecule detection level is practically reached if the deviation between  $\Pi(k; \bar{N}, \varepsilon, N_{\max} = 1)$  and  $\Pi(k; \bar{N}, \varepsilon, N_{\max} = 2)$  is equal to the experimental uncertainty. The lower limit of the

single-molecule detection level is reached if the deviation between the photon counting distribution  $\text{Poi}(\bar{k}, k)$  of the background signal and  $\Pi(k; \bar{N}, \varepsilon, N_{\max}=1)$  equals the experimental uncertainty. For instance, the lower detection limit is reached at  $\bar{N}=0.0057$  molecules ( $c=13$  pmol/l) while the upper single-molecule detection limit is reached at  $\bar{N}=0.048$  molecules ( $c=110$  pmol/l) for C153 excited at  $\lambda=800$  nm and  $\bar{P}=22$  mW ( $\varepsilon_T=12\,100$  cps). Furthermore, we studied the influence of the molecular brightness on the lower and on the upper detection limit.

## ACKNOWLEDGMENT

This research was supported by the Bundesministerium für Bildung und Forschung (BMBF) under Grant No. 13N7927.

- <sup>1</sup>R. Rigler and E. S. Elson, *Fluorescence Correlation Spectroscopy: Theory and Applications* (Springer, Berlin, 2001), pp. 305–330, pp. 411–437, and p. 438–458.
- <sup>2</sup>S. Nie and R. N. Zare, *Annu. Rev. Biophys. Biomol. Struct.* **26**, 567 (1997).
- <sup>3</sup>Y. Chen, J. D. Müller, Q. Ruan, and E. Gratton, *Biophys. J.* **82**, 133 (2002).
- <sup>4</sup>Y. Chen, L. Wie, and J. D. Müller, *Proc. Natl. Acad. Sci. U.S.A.* **100**, 15492 (2003).
- <sup>5</sup>A. A. Deniz, T. A. Laurence, M. Dahan, D. S. Chelma, P. G. Schultz, and S. Weiss, *Annu. Rev. Phys. Chem.* **52**, 233 (2001).
- <sup>6</sup>Y. Jung, E. Barkai, and R. J. Silbey, *J. Chem. Phys.* **117**, 10980 (2002).
- <sup>7</sup>R. Rigler, M. Orrit, and T. Basché, *Single Molecule Spectroscopy: Nobel Conference Lectures* (Springer, Berlin, 2001), pp. 130–144, pp. 227–256, and pp. 257–276.
- <sup>8</sup>T. Schmidt, G. J. Schütz, W. Baumgartner, H. J. Gruber, and H. Schindler, *J. Phys. Chem.* **99**, 17662 (1999).
- <sup>9</sup>G. S. Harms, L. Cognet, P. H. M. Lommerse, G. A. Blab, H. Kahr, R. Gamsjäger, H. P. Spaink, N. M. Soldatov, C. Romanin, and T. Schmidt, *Biophys. J.* **81**, 2639 (2001).
- <sup>10</sup>W. P. Ambrose, P. M. Goodwin, J. H. Jett, A. van Orden, J. H. Werner, and R. A. Keller, *Chem. Rev. (Washington, D.C.)* **99**, 2929 (1999).
- <sup>11</sup>R. Rigler, L. Edman, Z. Földes-Papp, and S. Wennmalm, *Single Molecule Spectroscopy: Nobel Conference Lectures* (Springer, Berlin, 2001), pp. 177–195.
- <sup>12</sup>M. Orrit, *Single Mol.* **3**, 255 (2002).
- <sup>13</sup>S. R. Aragon and R. Pecora, *J. Chem. Phys.* **64**, 1791 (1976).
- <sup>14</sup>C. Eggeling, A. Volkmer, and C. A. M. Seidel, *ChemPhysChem* **6**, 791 (2005); T. D. Perroud, B. Huang, and R. N. Zare, *ibid.* **6**, 905 (2005); T. Heinlein, A. Biebricher, P. Schlüter, C. M. Roth, D.-P. Herten, J. Wolfrum, M. Heilemann, C. Müller, P. Tinnefeld, and M. Sauer, *ibid.* **6**, 949 (2005); N. Baudendistel, G. Müller, W. Waldeck, P. Angel, and J. Langowski, *ibid.* **6**, 984 (2005).
- <sup>15</sup>K. G. Heinze, A. Koltermann, and P. Schwille, *Proc. Natl. Acad. Sci. U.S.A.* **97**, 10377 (2000).
- <sup>16</sup>C. Eggeling, J. Widengren, R. Rigler, and C. A. M. Seidel, *Anal. Chem.* **70**, 2651 (1998).
- <sup>17</sup>H. Qian and E. L. Elson, *Proc. Natl. Acad. Sci. U.S.A.* **87**, 5479 (1990).
- <sup>18</sup>Y. Chen, J. D. Mueller, J. S. Eid, and E. Gratton, in *New Trends in Fluorescence Spectroscopy: Applications to Chemical and Life Sciences*, edited by B. Valeur and J. Brochon (Springer, Berlin, 2001), pp. 292–295.
- <sup>19</sup>Y. Chen, J. D. Mueller, P. T. C. So, and E. Gratton, *Biophys. J.* **77**, 553 (1999).
- <sup>20</sup>J. D. Mueller, Y. Chen, and E. Gratton, *Biophys. J.* **78**, 474 (2000).
- <sup>21</sup>L. N. Hillesheim and J. D. Mueller, *Biophys. J.* **85**, 1948 (2003).
- <sup>22</sup>P. Kask, K. Palo, D. Ullmann, and K. Gall, *Proc. Natl. Acad. Sci. U.S.A.* **96**, 13756 (1999).
- <sup>23</sup>W. Denk, J. H. Strickler, and W. W. Webb, *Science* **248**, 73 (1990).
- <sup>24</sup>J. Mertz, C. Xu, and W. W. Webb, *Opt. Lett.* **20**, 2532 (1995).
- <sup>25</sup>T. D. Perroud, B. Huang, M. I. Wallace, and R. N. Zare, *ChemPhysChem* **4**, 1121 (2003).
- <sup>26</sup>T. D. Perroud and R. N. Zare, *ChemPhysChem* **5**, 1523 (2004).
- <sup>27</sup>R. Niesner, W. Roth, and K.-H. Gericke, *ChemPhysChem* **5**, 678 (2004).
- <sup>28</sup>A. Schönle, M. Glatz, and S. W. Hell, *Appl. Opt.* **39**, 6306 (2000).